A level-set method for computing the eigenvalues of elliptic operators defined on compact hypersurfaces

Jeremy Brandman [1]

Abstract

We demonstrate, through separation of variables and estimates from the semi-classical analysis of the Schrödinger operator, that the eigenvalues of an elliptic operator defined on a compact hypersurface in $\mathbb{R}^n$ can be found by solving an elliptic eigenvalue problem in a bounded domain $\Omega \subset \mathbb{R}^n$. The latter problem is solved using standard finite element methods on the Cartesian grid. We also discuss the application of these ideas to solving evolution equations on surfaces, including a new proof of a result due to Greer (J. Sci. Comput. 29(3) 2006).

1 Introduction

In this paper we demonstrate that the eigenvalues of an elliptic operator

$$-\nabla_S \cdot (a(x)\nabla_S u) = \lambda u \quad \text{for all} \quad x \in \Sigma \tag{1}$$

defined on a compact hypersurface $\Sigma \subset \mathbb{R}^n$ can be found by solving a related elliptic eigenvalue problem $Lu = \lambda u$ on a rectangular domain in $\mathbb{R}^n$. Here, ∇_S is the surface gradient operator and $\nabla_S \cdot$ the surface divergence operator. From a computational point of view, there are at least three benefits to this approach.

- **Simplicity.** No triangularization of Σ is needed. Σ is represented implicitly as the zero level-set of a function ϕ and geometric quantities of interest related to Σ, such as the directions of principal curvature, are calculated using standard finite differences on the Cartesian grid.
- **Ease of implementation.** One finds the eigenvalues by solving a standard finite element problem on the Cartesian grid.
- **Dependence on reliable numerical schemes.** The finite element method has well-known convergence rate estimates for the eigenfunctions and eigenvalues of elliptic problems [19].

Fast, accurate, and reliable methods for solving (1) are of interest in shape analysis and medical imaging. In recent years, several numerical studies have been carried out investigating how effectively the spectrum of the Laplace-Beltrami operator characterizes surfaces [17]. The methods used in these studies typically rely on a triangulation or parametrization of the surface. Such an approach is taken in [17]; in the words of the authors:

"Even though this method seems to be very simple, it is quite tricky to implement" [17], p. 352.

[1]Department of Mathematics, University of California Los Angeles, Los Angeles, CA, 90095, email: jbrandma@math.ucla.edu

Our conversion of (1) to an eigenvalue problem defined in a domain containing Σ is motivated by the success of the level-set method in computing moving fronts and solving PDE on surfaces. The level-set method was introduced in [16] as a numerical method for tracking interfaces. From a computational point of view, the effectiveness of the method comes from its conversion of front-tracking problems to PDE which can be solved using standard numerical methods. Given an initial interface $\Gamma(0) = \{x : \phi(x, 0) = 0\}$ and a velocity law for the evolution of the interface, the level-set method evolves $\Gamma(0)$ by first finding $g : \Omega \to \mathbb{R}$ such that $\Gamma(0) = \{x : g(x) = 0\}$ and then solving

$$\phi_t + \vec{v} \cdot \nabla\phi = 0 \ \text{ in } \ \Omega \ \text{ such that } \ \phi(\cdot, t = 0) = g(\cdot) \tag{2}$$

in a domain containing the interface. In (2), the velocity $\vec{v}$ represents an extension of the velocity law by which the interface is known to evolve. The interface is recovered at each time t through the formula $\Gamma(t) = \{x : \phi(x, t) = 0\}$. By solving (2) on the Cartesian grid, interface motion is computed without explicitly tracking points on the interface. For this reason, the level-set method is considered an Eulerian approach to interface tracking.

Level-set methods for solving PDE on surfaces were introduced in [2]. Rather than solving such equations directly via triangulation or parametrization of the surface, the authors represent the surface as the zero level set of a function ψ and solve a related problem using finite differences in a domain containing the surface. The solution to the domain problem solves the appropriate surface PDE on each level set simultaneously. Using this approach, equations such as

$$u_t = \Delta_S u \ \text{ and } \ u_t = \nabla_S \cdot \left(\frac{\nabla_S u}{|\nabla_S u|} \right).$$

are solved using finite differences on the Cartesian grid and applied to problems in image processing. As an example, the solution to $u_t = \Delta_S u$ is found by solving

$$u_t = \frac{1}{|\nabla\psi|} \nabla \cdot (P_{\nabla\psi} \nabla u |\nabla\psi|) \tag{3}$$

in a domain containing the surface. Since $P_{\nabla\psi}$ is the projection $I - \frac{\nabla\psi \otimes \nabla\psi}{|\nabla\psi|^2}$ and ψ is a level-set function of Σ, all quantities needed to solve the above equation can be computed easily and accurately using finite differences. It can be shown [4] that the solution to (3) solves the heat equation on each level-set of ψ. We see in this example, as well as in the level-set approach to (2), that problems originally defined on surfaces may be extended to problems defined on domains using implicit surfaces. The advantage of this approach is that sometimes the domain problem can be solved using standard numerical schemes, such as finite difference methods.

The methods introduced in [2] were applied to the computation of geodesics, Wulff shapes, and other objects in [4]. Martin Burger extended the framework of [2] to solve elliptic PDE, including those of the form

$$-\nabla_S \cdot (a \nabla_S u) + cu = f, \tag{4}$$

using finite elements in [3]. Given a level-set function ψ of Σ, Burger demonstrates that the solution of (4) can be found as the restriction to Σ of the function u^* which solves (4) on each level-set of ψ in a domain $\Omega \supset \Sigma$, subject to a Neumann boundary condition. Applying

integration by parts and the co-area formula, Burger shows that u^* is the unique function satisfying

$$\int_\Omega A\langle P_{\nabla\psi}\nabla u, P_{\nabla\psi}\nabla v\rangle + Cuv\ dx = \int_\Omega Fv\ dx \tag{5}$$

for all test functions v in the appropriate Sobolev space. Here $A(x) = \hat{a}(x)|\nabla\psi(x)|$, $C(x) = \hat{c}(x)|\nabla\psi(x)|$, $F(x) = \hat{f}(x)|\nabla\psi(x)|$, and $\hat{a}, \hat{c}, \hat{f} : \Omega \to \mathbb{R}$ are extensions of the functions $a, c, f : \Sigma \to \mathbb{R}$. Using this weak formulation, Burger solves for u^* using the finite element method with a highly adaptive mesh which is fine near Σ and coarse far from Σ. This approach provided some motivation for the weak formulation of our problem found in section 2.2.

The remainder of this paper is organized as follows. In Section 2.1, we construct an elliptic differential operator L, defined in a tubular neighborhood Σ_δ of Σ, with the property that the eigenvalues of

$$Lu = \lambda u \ \text{ in } \ \Sigma_\delta \ \text{ and } \ u = 0 \ \text{ on } \ \partial\Sigma_\delta \tag{6}$$

are $\{\lambda_m^\Sigma + \lambda_j^r\}_{j,m=1}^\infty$. Here, $\{\lambda_m^\Sigma\}_{m=1}^\infty$ are the eigenvalues of (1) and $\{\lambda_j^r\}_{j=1}^\infty$ are the eigenvalues of a known one dimensional problem. This result is established by separation of variables, with motivation coming from the relation between the spherical harmonics, which are eigenfunctions of the surface Laplacian on S^{n-1}, and the eigenfunctions of the Laplacian in $\{x \in \mathbb{R}^n : |x| < 1\}$ subject to zero Dirichlet data [1, 6]. We proceed, in Section 2.2, to introduce a weak formulation of (6), which we use for our numerical implementation.

In Section 3, we prove our main result, which demonstrates the existence of an elliptic differential operator L, defined in an arbitrary domain Ω containing Σ, having the property that the eigenvalues of

$$Lu = \lambda u \quad \text{ in } \ \Omega \ \text{ and } \ u = 0 \ \text{ on } \ \partial\Omega \tag{7}$$

are approximately $\{\lambda_m^\Sigma + \lambda_j^r\}_{j,m=1}^\infty$. This result extends the ideas from Section 2.1 to a more general setting and demonstrates that the eigenvalues of (1) can be found numerically by discretizing (7) on the Cartesian grid. The key idea is to design L in such a way that eigenfunctions corresponding to small eigenvalues decay rapidly to zero away from Σ; it then follows from the spectral theory of self-adjoint operators that the eigenvalues of (7) are close to those of (6), for the same differential operator L, and the result follows. Using estimates from the semi-classical analysis of the Schrödinger operator [13], we make this rigorous in the case where L has a large single well potential concentrated near Σ.

In Section 4, we outline a simple finite element method for solving (7) based on the weak formulation from section 2.2 and discuss different approaches to calculating the eigenvalues of (1) from those of (7). Numerical results in two and three space dimensions, obtained by solving (7) on a square (2-D) or cube (3-D), are presented in Section 5. Future challenges are discussed in Section 6. We examine applications of the results from Section 2.1 to the numerical solution of evolution equations on Σ in Appendices A and B. Appendix A contains a simplified proof of a special case of the main result from [11] and Appendix B contains useful formulas. In Appendix C we collect some results from spectral theory which are used in Section 3.

2 Local analysis

We use the following notation throughout the paper.

Notation.

- $\langle \cdot, \cdot \rangle$ = Euclidean inner product.
- $\mathbb{R}^n \supset \Sigma$ = compact hypersurface.
- Ω = domain containing Σ.
- ϕ = signed distance function to Σ; $\phi < 0$ inside of Σ.
- $\Sigma_\delta = \{x : |\phi(x)| < \delta\}$.
- $P_x v = v - \langle \nabla\phi(x), v \rangle \nabla\phi(x)$ = projection of v onto $(\nabla\phi(x))^\perp$.
- ∇_S = surface gradient on Σ.
- $\nabla_S \cdot$ = surface divergence on Σ.

2.1 Separation of variables

In this section, we relate the eigenfunctions $\{f_n\}$ and eigenvalues $\{\lambda_n^\Sigma\}$ of (1) to the eigenvalues of (6) using a separation of variables argument. Here, L is an elliptic operator in Σ_δ which we define later and the separation of variables is performed by looking for eigenfunctions of L which factor into the product of an eigenfunction of (1) and an eigenfunction of a one dimensional problem related to L. In order to guarantee that the original eigenvalue problem (1) is elliptic, we assume throughout this paper that

$$a \in L^\infty(\Sigma) \quad \text{and} \quad a \geq c > 0. \tag{8}$$

The main result of this section is Theorem 2.1, which states that the functions $\{f_n \cdot g_m\}_{n,m=1}^\infty$, where $\{g_m\}$ is a basis of eigenfunctions for a related one dimensional problem, form a complete set of eigenfunctions for (6). As a result, the eigenvalues of (6) are $\{\lambda_n^\Sigma + \lambda_m^r\}_{n,m=1}^\infty$, where $\{\lambda_m^r\}$ are the eigenvalues of the one dimensional problem. Later in this section, we clarify what is meant by the expression $f_n \cdot g_m$. In Section 3, we extend Theorem 2.1 to more general domains, providing justification for the numerical method presented in Section 4.

Our first step towards proving Theorem 2.1 is to define L and examine some of its properties. In order to define L, we first mention some basic facts regarding the geometry of Σ_δ and the formulation of these facts in terms of the signed distance function ϕ. The most important of these is that for δ appropriately small, each $x \in \Sigma_\delta$ can be written uniquely as

$$x = s + \phi(x)\nu(s), \quad \text{where } s \in \Sigma \text{ and } \nu(s) = \text{ outer unit normal at s [10]}. \tag{9}$$

This decomposition can be written in terms of ϕ as

$$x = (x - \phi(x)\nabla\phi(x)) + \phi(x)\nabla\phi(x).$$

We may also express the operator ∇_S easily using ϕ. For $x \in \Sigma$ and smooth u defined in a neighborhood of Σ, we have that

$$\nabla_S u(x) = \nabla u - \langle \nabla u(x), \nabla \phi(x) \rangle \nabla \phi(x).$$

We are now nearly ready to define the linear differential operator L, which we write as $L = L_\Sigma + L_n$. The operators L_Σ and L_n are defined so that if $h(x) = f(x - \phi(x)\nabla\phi(x)) \cdot g(\phi(x))$, then

$$L_\Sigma(h) = g \cdot L_\Sigma(f) \text{ and } L_n(h) = f \cdot L_n(g). \tag{10}$$

We impose this requirement on L_Σ and L_n in order to perform the separation of variables used in the proof of Theorem 2.1. We make some preliminary definitions.

Definition 2.1. If $u : \Sigma_\delta \to \mathbb{R}$ is a smooth function, we define the function $u^r : \Sigma \to \mathbb{R}$ according to $u^r(s) := u(s + r\nabla\phi(s))$. We then set $(\nabla_S^r u)(s) := (\nabla_S u^r)(s)$ for $s \in \Sigma$.

Geometrically, one obtains u^r by taking the restriction of u to the r level-set and projecting it onto Σ using (9). We can express $(\nabla_S^r u)$ using the chain rule as

$$(\nabla_S^r u)(s) = P_{\nabla\phi(s)} \left[\nabla u|_{s + r\nabla\phi(s)} (I + rD^2\phi(s)) \right]. \tag{11}$$

We now define L_Σ and L_n by describing their action on smooth functions.

Definition 2.2. (Definition of L_Σ and L_n) For any $x \in \Sigma_\delta$ and smooth function $u : \Sigma_\delta \to \mathbb{R}$, $L_n(u)$ and $L_\Sigma(u)$ are calculated according to

$$L_n(u) \mid_x = -\langle D^2 u(x) \nabla\phi(x), \nabla\phi(x) \rangle + \frac{1}{\epsilon^2} \cdot (\phi(x))^2 u(x)$$

and

$$L_\Sigma(u) \mid_x = -\nabla_S \cdot \left(a \nabla_S \left(u^{\phi(x)} \right) \right) \mid_{x - \phi(x)\nabla\phi(x)}.$$

In section 3 we discuss the significance of the $\frac{1}{\epsilon^2}$ parameter appearing in the definition of L_n. The analysis performed here is independent of ϵ. It follows from (9) that for smooth functions u

$$\langle D^2 u(x) \nabla\phi(x), \nabla\phi(x) \rangle = \frac{d^2}{dr^2} u(x + r\nabla\phi(x)) \mid_{r=0}.$$

From this, we see that L_n is a second-order differential operator acting only in the normal direction to Σ, while from Definition 2.2 we see that L_Σ is a second-order differential operator acting only "along Σ". In Example 2.1, we compute u^r, $\nabla_S^r u$, $L_n(u)$, and $L_\Sigma(u)$ in a particular case.

Example 2.1

Let $\Sigma = S^1$, so that $\phi(x) = |x| - 1$, and set $a :\equiv 1$. In this case, it can be shown that

$$L_\Sigma = -\frac{d^2}{d\theta^2} \quad \text{and} \quad L_n = -\frac{d^2}{dr^2} + \frac{1}{\epsilon^2}(r-1)^2.$$

Define the function $u : \mathbb{R}^2 \to \mathbb{R}$ using polar coordinates according to $u(r,\theta) = r^2\cos\theta$. Identifying the point $(\cos\theta, \sin\theta)$ with $\theta \in [0, 2\pi)$, it follows from Definition 2.1 that

$$u^l(\theta) = (l+1)^2\cos\theta \quad \text{and} \quad (\nabla_S^l u)(\theta) = -(l+1)^2\sin\theta(-\sin\theta, \cos\theta).$$

We use these calculations to find that

$$L_\Sigma u\,|_{(r,\theta)} = r^2\cos\theta \quad \text{and} \quad L_n u\,|_{(r,\theta)} = -2\cos\theta + \frac{1}{\epsilon^2}(r-1)^2 r^2\cos\theta.$$

We now show that L_n and L_Σ satisfy (10).

Proposition 2.1. (L separates variables) If $h(x) = f(x - \phi(x)\nabla\phi(x))g(\phi(x))$, then $L_\Sigma(h) = g \cdot L_\Sigma(f)$ and $L_n(h) = f \cdot L_n(g)$.

Proof. the result follows directly from Definition 2.2. □

Applying Proposition 2.1 in the case $u(x) = f_n(x - \phi(x)\nabla\phi(x))$, where f_n is an eigenfunction of (1) with eigenvalue λ_n, we find that $L_\Sigma u = \lambda_n u$ and $L_n u = \frac{1}{\epsilon^2}(\phi)^2 u$. We now use Proposition 2.1 to prove Theorem 2.1, which relates the eigenvalues and eigenfunctions of (6) to those of (1). Theorem 2.1 forms the basis of our numerical method, since it shows how the eigenfunctions and eigenvalues of (1) can be computed from those of L with zero Dirichlet boundary data.

Theorem 2.1. Let Σ_δ be such that (9) holds at every point. Then the eigenvalues $\{\lambda_{m,n}\}_{m,n=1}^\infty$ and eigenfunctions $\{h_{m,n}\}_{m,n=1}^\infty$ of (6) factor and sum, respectively:

$$h_{m,n}(x) = f_n(x - \phi(x)\nabla\phi(x))g_m(\phi(x))$$

$$\lambda_{m,n} = \lambda_n^\Sigma + \lambda_m^r.$$

Here, the $\{f_n\}$ are eigenfunctions of (1) and form an orthonormal basis for $L^2(\Sigma)$, while the $\{\lambda_n^\Sigma\}$ are the corresponding eigenvalues. The $\{g_m\}$ are eigenfunctions of the one-dimensional problem

$$-y''(t) + \frac{1}{\epsilon^2}\cdot t^2 y(t) = \lambda y \quad \text{for } t \in (-\delta, \delta) \quad \text{and } y(-\delta) = y(\delta) = 0 \tag{12}$$

and form an orthonormal basis for $L^2((-\delta,\delta))$, while the $\{\lambda_m^r\}$ are the corresponding eigenvalues.

Proof. We assume that a is smooth; by working with the weak form of the problem, discussed in Section 2.2, we can prove the result for rougher a. First note that we may express any eigenfunction u as

$$u(x) = \sum_{n=0}^\infty f_n(x - \phi(x)\nabla\phi(x))k_n(\phi(x)) \tag{13}$$

for some functions $\{k_n\}$, since the $\{f_n\}$ form an orthonormal basis of $H^1(\Sigma)$ [18]. Since L is elliptic (see Corollary 8.1), any eigenfunction $u \in C^\infty(\bar{\Sigma_\delta})$ [7] and uniformly rapid decay

of the $\{k_n\}$ (with respect to ϕ) follows from integration by parts. This decay allows us to differentiate (13) term by term pointwise and, applying Proposition 2.1, we find that

$$Lu = \sum_{n=0}^{\infty} \lambda_n^{\Sigma} f_n k_n - f_n k_n'' + \frac{1}{\epsilon^2}(\phi^2) f_n k_n.$$

Since by hypothesis $Lu = \lambda u$, we then have

$$\sum_{n=0}^{\infty} \lambda_n^{\Sigma} f_n k_n - f_n k_n'' + \frac{1}{\epsilon^2}(\phi^2) f_n k_n = \lambda \sum_{n=0}^{\infty} f_n k_n$$

and the result follows. □

We remark here that the design of L was motivated by the solution of the eigenvalue problem

$$-\Delta u = \lambda u \quad x \in \{z \in \mathbb{R}^3 : |z| < 1\} \text{ such that } u = 0 \text{ for } x \in S^2. \tag{14}$$

Separating variables and looking for eigenfunctions of the form

$$f(x) = g\left(\frac{x}{|x|}\right) h(|x|)$$

we find [1, 6] that $g : S^2 \to \mathbb{R}$ is a spherical harmonic, i.e. it satisfies, for a constant α,

$$-\Delta_S g = \alpha g \quad x \in S^2,$$

while $h : [0, 1] \to \mathbb{R}$ is a function which is regular at $r = 0$ and satisfies

$$(r^2 h')' - \alpha h + \lambda r^2 h = 0 \text{ and } h(1) = 0.$$

This demonstrates that (14) can be reduced to solving an eigenvalue problem on the unit sphere and another one on an interval. Our approach to (1) proceeds in the opposite direction, since we convert a problem originally defined on Σ into one defined in a domain. We are faced with additional complications which do not arise in the study of (14) since we make no assumptions on the curvature of Σ. While it may appear that our approach complicates the matter, our goal is to convince the reader that it yields computational benefits.

2.2 Weak formulation

We now provide a weak formulation of (7) valid for domains Ω which are not necessarily tubular neighborhoods of Σ but in which (9) holds. We use this weak form in Section 4 to solve a modified version of (6) numerically using the finite element method. Our first step is to introduce an inner product, which we denote by $(\cdot, \cdot)_\Omega$, in which L is symmetric. This is the content of Definition 2.3 and Proposition 2.2. All definitions in this section are given for domains in which (9) holds.

Definition 2.3. Let u and v be bounded functions. We define $(u,v)_\Omega$ by the formula

$$(u,v)_\Omega = \int_{-\infty}^{\infty} \int_{\Omega \bigcap \{x:\phi(x)=r\}} u(s + r\nabla\phi(x))v(s + r\nabla\phi(x))\ dS(s)\ dr.$$

Here, dS is surface measure on Σ. Using the notation introduced in Definition 2.2, the above can be rewritten as

$$(u,v)_\Omega = \int_{-\infty}^{\infty} \int_{\Omega \bigcap \{x:\phi(x)=r\}} u^r(s)v^r(s)\ dS(s)\ dr.$$

The inner product $(\cdot,\cdot)_\Omega$ can be written as a weighted $L^2(\Omega)$ inner product. Before we give the general result, we consider a special case.

Example 2.2.

Let $\Sigma = S^{n-1}$ and $\Omega = \mathbb{R}^n$. By a change of variables, we have

$$(u,v)_\Omega = \int_0^{\infty} \int_{S^{n-1}} u(rs)v(rs)\ dS(s)\ dr$$

which can be rewritten as

$$(u,v)_\Omega = \int_{\mathbb{R}^n} \frac{u(x)v(x)}{|x|^{n-1}}\ dx.$$

The following result is a generalization of Example 2.2 to smooth surfaces Σ.

Proposition 2.2. Suppose that (9) holds inside Ω. For $x \in \Omega$, let $\{\kappa_i(x)\}_{i=1}^{n-1}$ be the principal curvatures of the level-set $\phi(x)$ at x and let u and v be bounded measurable functions. Then

$$(u,v)_\Omega = \int_\Omega \left[\prod_{i=1}^{n-1}(1 - \phi(x)\kappa_i(x))\right] u(x)v(x)\ dx \tag{15}$$

The proof relies on (9) and consists of an application of the coarea formula and a formula relating surface measure on $\{x : \phi(x) = r\}$, dS_r, to dS. We relate dS_r to dS in the following lemma.

Lemma 2.1. Let dS_r be surface measure on $\{x : \phi(x) = r\}$. Then

$$dS_r(x) = \left[\prod_{i=1}^{n-1}(1 - \phi(x)\kappa_i(x))\right]^{-1} dS(x - r\nabla\phi(x)).$$

Proof. If $\gamma(u_1, ..., u_{n-1})$ is a local parameterization of Σ, then $\gamma(u_1, ...u_{n-1}) + r\nabla\phi(\gamma(u_1, ..., u_{n-1}))$ is a local parametrization of $\{x \in \mathbb{R}^n : \phi(x) = r\}$. For vectors $v = (v_1, ...v_{n-1})$ we define $A(v)$ as the matrix with columns $\{\gamma_{u_1}(v), ..., \gamma_{u_{n-1}}(v)\}$; it follows that dS is given locally by

$$dS(\gamma(u)) = \left[\det\ (A(u) \cdot A(u)^t)\right]^{1/2}\ du_1...du_{n-1}$$

and dS_r is given locally by

$$dS_r(\gamma(u) + r\nabla\phi(\gamma(u))) = \left[\det\ ((I + r \cdot D^2\phi)(A)(A^t)(I + r \cdot D^2\phi)^t)\right]^{1/2}\ du_1...du_{n-1}$$

$$= \det[I + r \cdot D^2\phi(\gamma(u))]\ dS. \tag{16}$$

We now rewrite (16) in terms of the principal curvatures of Σ at $\gamma(u)$. Recall that $D^2\phi(\gamma(u))$ is the Gauss map of Σ at $\gamma(u)$ and so can be written as [14]

$$D^2\phi(\gamma(u)) = \begin{pmatrix} \kappa_1(\gamma(u)) & & & & \\ & \kappa_2(\gamma(u)) & & & \\ & & \cdot & & \\ & & & \cdot & \\ & & & \kappa_{n-1}(\gamma(u)) & \\ & & & & 0 \end{pmatrix} \tag{17}$$

with respect to the basis $\{e_1, ..., e_{n-1}, \nabla\phi\}$, where the $\{e_i\}$ are directions of principal curvature. Substituting (17) into (16), we find that

$$dS_r = \left[\prod_{i=1}^{n-1}(1 + r\kappa_i(\gamma(u)))\right]\ du_1...du_{n-1} \tag{18}$$

Next, recall the following relationship between the principal curvatures $\{\kappa_i\}$ at the points $x \in \Sigma$ and $x + r\nabla\phi(x)$ [10]:

$$\kappa_i(x + r\nabla\phi(x)) = \frac{\kappa_i(x)}{1 + r\kappa_i(x)} \tag{19}$$

We can establish (19) by differentiating the identity

$$\nabla\phi(x) = \nabla\phi(x + r\nabla\phi(x))$$

to arrive at

$$D^2\phi(x) = D^2\phi(x + r\nabla\phi(x))[I + rD^2\phi(x)].$$

Substituting (19) into (18), the lemma is proven. □

Proof of Proposition 2.2. Use Lemma 2.1 to rewrite the integrals over Σ which define $(\cdot,\cdot)_\Omega$ as integrals over level-sets $\{x : \phi(x) = r\}$. Recalling that $|\nabla\phi(x)| \equiv 1$ for $x \in \Omega$, the proposition then follows from the co-area formula [1, 8, 22]. □

The key feature of $(\cdot,\cdot)_\Omega$ is that L is symmetric with respect to it. This follows from integration by parts, as we now show.

Proposition 2.3. Suppose that (9) holds inside Ω. Then L is symmetric with respect to $(\cdot,\cdot)_\Omega$: if $u, v \in C_c^2(\Omega)$, then $(Lu, v)_\Omega = (u, Lv)_\Omega$.

Proof. Applying Fubini's theorem and the divergence theorem for Riemannian manifolds, we integrate by parts and find that $(Lu, v)_\Omega$ equals

$$\int_{-\infty}^{\infty} \int_{\Omega \bigcap \{x:\phi(x)=r\}} a(s)\langle \nabla_S^r u, \nabla_S^r v\rangle + \left(\frac{\partial}{\partial r} u \cdot \frac{\partial}{\partial r}\ v\right) |_{s+r\nabla\phi(s)} + \frac{1}{\epsilon^2} \cdot r^2 u^r(s) v^r(s)\ dS(s)\ dr. \quad (20)$$

which is symmetric in u and v. In the above, $\frac{\partial}{\partial r} u = \langle \nabla u, \nabla \phi \rangle$. □

Note that the above integration by parts could not be performed if we worked with the standard L^2 inner product on Ω. Motivated by Proposition 2.3, we define the following function space and bilinear form used for a weak formulation of (7).

Definition 2.4. For $u \in C^2(\bar{\Omega})$, we set

$$\|u\|_\Omega^2 := (Lu, u)_\Omega \quad \text{and} \quad a(u, v)_\Omega := (Lu, v)_\Omega.$$

We define $W(\Omega)$ to be the closure of $C_c^2(\Omega)$ with respect to $\| \cdot \|_\Omega$.

We now give the weak formulation of (7). In Section 4, we use this formulation to solve (7) using the finite element method.

Definition 2.5. $u \in W(\Omega)$ is a weak solution of (7) if

$$a(u, v)_\Omega = \lambda(u, v)_\Omega \quad \text{for all} \quad v \in W(\Omega). \quad (21)$$

The following example demonstrates how to express $a(\cdot, \cdot)_\Omega$ as an integral over Ω. We use a modified version of this expression for $a(\cdot, \cdot)_\Omega$ in Section 4 when we solve (7) using the finite element method. A discussion of these modifications can be found in a remark after the example.

Example 2.3.

In this example, we use (11) and Proposition 2.2 to write $a(\cdot, \cdot)_\Omega$ as an integral over Ω. For simplicity, we work in three space dimensions. We assume the domain of definition of a has been extended to Ω by defining the function a to be constant along normals to Σ:

$$a(x) = a(x - \phi(x)\nabla\phi(x)) \quad \text{for} \quad x \in \Omega. \quad (22)$$

Recalling (20), we break up $a(u, v)$ according to

$$\int_{-\infty}^{\infty} \int_{\Omega \cap \{x:\phi(x)=r\}} a(s)\langle \nabla_S^r u, \nabla_S^r v\rangle + \frac{\partial}{\partial r} u|_{s+r\nabla\phi(s)} \cdot \frac{\partial}{\partial r}\ v|_{s+r\nabla\phi(s)} + \frac{1}{\epsilon^2} \cdot r^2 u^r(s) v^r(s)\ dS(s)\ dr$$

$$= I + II + III.$$

It follows immediately from Proposition 2.2 that

$$II = \int_\Omega \left[(1 - \phi(x)\kappa_1(x))(1 - \phi(x)\kappa_2(x))\right] \langle \nabla u(x), \nabla\phi(x)\rangle \langle \nabla v(x), \nabla\phi(x)\rangle\ dx.$$

Next, we express I as an integral over Ω. Let $\{e_1(x), e_2(x)\}$ be the directions of principal curvature for the $\phi(x)$ level-set at the point x. Since the directions of principal curvature at x are the same as those at $x - \phi(x)\nabla\phi(x)$ [10], we apply (17) and (11) to find that

$$(\nabla_S^r u)(s) = (1 + r\kappa_1(s))\langle \nabla u|_{s+r\nabla\phi}, e_1\rangle e_1 + (1 + r\kappa_2(s))\langle \nabla u|_{s+r\nabla\phi}, e_2\rangle e_2.$$

Using (19) to rewrite the above expression in terms of the $\{\kappa_i(x)\}$, it follows from Proposition 2.2 that

$$I = \int_\Omega a(x)\frac{1-\phi(x)\kappa_2(x)}{1-\phi(x)\kappa_1(x)}\langle \nabla u(x), e_1\rangle\langle \nabla v(x), e_1\rangle + a(x)\frac{1-\phi(x)\kappa_1(x)}{1-\phi(x)\kappa_2(x)}\langle \nabla u(x), e_2\rangle\langle \nabla v(x), e_2\rangle \, dx.$$

Remark 2.1. in practice, we often work in domains for which (9) does not hold everywhere. In such cases, we solve a modified form of (21), which comes from regularizing $(\cdot,\cdot)_\Omega$ and $a(\cdot,\cdot)_\Omega$. Justification for this regularization is found in Section 3. Using the notation from the previous example, we regularize $a(\cdot,\cdot)_\Omega$ according to

$$I = \int_\Omega a(x)\frac{|1-\phi(x)\kappa_2(x)|}{|1-\phi(x)\kappa_1(x)| + \alpha}\langle \nabla u(x), e_1\rangle\langle \nabla v(x), e_1\rangle \, dx$$

$$+ \int_\Omega a(x)\frac{|1-\phi(x)\kappa_1(x)|}{|1-\phi(x)\kappa_2(x)| + \alpha}\langle \nabla u(x), e_2\rangle\langle \nabla v(x), e_2\rangle \, dx$$

and

$$II = \int_\Omega |(1-\phi(x)\kappa_1(x))(1-\phi(x)\kappa_2(x))|\langle \nabla u(x), \nabla\phi(x)\rangle\langle \nabla v(x), \nabla\phi(x)\rangle \, dx.$$

Here, $\alpha << 1$ is a small parameter used to avoid division by zero. We introduce absolute value signs in order to ensure the positivity of $(u,u)_\Omega$ and $a(u,u)_\Omega$. The regularized bilinear form is computed easily using standard finite differences on the Cartesian grid.

3 Global analysis

In this section we prove Theorem 3.1, an extension of Theorem 2.1 to smooth domains $\Omega \supset \Sigma$ in which (9) may not hold everywhere. An important consequence of Theorem 3.1, which we pursue in sections 4 and 5, is that the eigenvalues of (1) can be found numerically by solving certain elliptic eigenvalue problems defined on a square (2-D) or cube (3-D) containing Σ.

Because we work with general smooth domains $\Omega \supset \Sigma$ for which (9) does not necessarily hold, the differential operator L may not be well-defined throughout our domain. For this reason, we consider in this section the eigenvalue problem $\tilde{L}u = \lambda u$ where $\tilde{L}$ represents an extension of L to Ω. We assume this eigenvalue problem can be written as

$$\tilde{L}u := -\frac{1}{w(x)}\sum_{i,j=1}^{n}(b_{ij}u_{x_j})_{x_i} + \frac{1}{\epsilon^2}\psi^2(x)u = \lambda u \ \text{ in } \ \Omega \ \text{ and } \ u = 0 \ \text{ on } \ \partial\Omega \qquad (23)$$

and make several assumptions regarding the coefficients of $\tilde{L}$. In Appendix B, we demonstrate how to write L in divergence form. In order that weak solutions of (23) satisfy (23) pointwise

a.e., we assume that the coefficients $b_{ij} : \Omega \to \mathbb{R}$ are Lipschitz continuous, $\psi : \Omega \to \mathbb{R}$ is a bounded measurable function, and $w : \Omega \to \mathbb{R}$ is a bounded measurable function which also satisfies $w(x) \geq c > 0$. We also assume that $b_{ij} = b_{ji}$ and

$$c_1|\xi|^2 \leq \sum_{i,j=1}^{n} b_{ij}\xi_i\xi_j \leq c_2|\xi|^2 \text{ in } \Omega$$

so that $\tilde{L}$ is an elliptic operator which is self-adjoint with respect to the inner product

$$\langle u, v\rangle_{L^2(\Omega,w)} = \int_\Omega w(x)u(x)v(x)\, dx.$$

Our final assumption is that $\tilde{L} = L$ in Σ_{δ^*} for some $\delta^* > 0$ and $\psi(x) \cdot \phi(x) \geq 0$ for all $x \in \Omega$, with equality only on Σ.

Throughout this section, $\{\lambda_j^\epsilon(\Omega)\}_{j=1}^\infty$ refers to the eigenvalues of (23) and $\{\lambda_j^\epsilon(\Sigma_{\delta^*})\}_{j=1}^\infty$ the eigenvalues of (6). We let $\{u_j^\epsilon(\Omega)\}_{j=1}^\infty$ be a set of eigenfunctions of (23) which form an orthonormal basis of $L^2(\Omega)$ with respect to $\langle\cdot,\cdot\rangle_{L^2(\Omega,w)}$ and $\{u_j^\epsilon(\Sigma_{\delta^*})\}_{j=1}^\infty$ be a set of eigenfunctions of (6) which form an orthonormal basis of $L^2(\Sigma_{\delta^*})$ with respect to $\langle\cdot,\cdot\rangle_{L^2(\Sigma_{\delta^*},w)} = (\cdot,\cdot)_{\Sigma_{\delta^*}}$.

We now state our main result.

Theorem 3.1. Let $\Omega \supset \Sigma$ be a smooth domain. For each $j \in \mathbb{N}$, $\lambda_j^\epsilon(\Omega) \to \frac{1}{\epsilon} + \lambda_j^\Sigma$ as $\epsilon \to 0$ in the sense that

$$\lim_{\epsilon\to 0} \left|\lambda_j^\epsilon(\Omega) - \left(\frac{1}{\epsilon} + \lambda_j^\Sigma\right)\right| \cdot e^{\frac{D_j}{\epsilon}} = 0$$

for some constant $D_j > 0$.

The first step in the proof of Theorem 3.1 is to show that, as $\epsilon \to 0$ in (23), the eigenvalues of (23) become exponentially close to those of (6) for $\delta = \delta^*$. This is the content of Lemmas 3.1 and 3.2, the proofs of which depend heavily on the rapid decay of the eigenfunctions of (23) to zero away from Σ. These lemmas use the decay estimates from the semiclassical analysis of the Schrödinger operator stated in Proposition C.4. The second step of the proof of Theorem 3.1 is to establish, using Theorem 2.1, that as $\epsilon \to 0$ the eigenvalues of (6) are approximately $\frac{1}{\epsilon} + \lambda_j^\Sigma$. This is the content of Lemma 3.3.

Remark 3.1. The effect of the single well potential can be seen graphically in Figure 12.

Proof of Theorem 3.1. We break the proof up into the three lemmas mentioned above. Throughout, we refer to results from Appendix C. Our first result bounds the distance between each eigenvalue of (23) and the spectrum of (6).

Lemma 3.1. Let $\text{spec}(L|_{\Sigma_{\delta^*}})$ be the set of eigenvalues of (6). There exists positive constants C_j and D_j such that

$$\text{dist}\left(\lambda_j^\epsilon(\Omega), \text{spec}(L|_{\Sigma_{\delta^*}})\right) \leq C_j e^{-D_j/\epsilon}. \tag{24}$$

Proof. Let $\chi \in C^\infty(\mathbb{R})$ be a smooth cutoff function such that $\chi \equiv 1$ for $x \in [-\delta^*/2, \delta^*/2]$ and $\chi \equiv 0$ for $|x| \geq \delta^*$. By Lemma 3.3 and Proposition C.1 we have that

$$\lambda_j^\epsilon(\Omega) \leq \lambda_j^\epsilon(\Sigma_{\delta^*}) \leq K_j \left(\frac{1}{\epsilon} + \lambda_j^\Sigma \right). \tag{25}$$

It then follows from Proposition C.4 that there exists positive constants C_j and D_j such that

$$\|\chi \cdot u_j^\epsilon(\Omega)\|_{L^2(\Sigma_{\delta^*}, w)} \geq 1 - C_j e^{-D_j/\epsilon}. \tag{26}$$

Estimates (25) and (26), along with standard estimates for second order elliptic PDE [10], imply that

$$\|(L - \lambda_j^\epsilon(\Omega))(\chi \cdot u_j^\epsilon(\Omega))\|_{L^2(\Sigma_{\delta^*}, w)} \leq C_j e^{-D_j/\epsilon}.$$

Proposition C.2, applied to $L : H^2(\Sigma_\delta) \cap H_0^1(\Sigma_\delta) \to L^2(\Sigma_\delta)$, then implies that

$$\operatorname{dist}(\lambda_j^\epsilon(\Omega), \operatorname{spec}(L|_{\Sigma_{\delta^*}})) \leq \frac{C_j e^{-D_j/\epsilon}}{1 - C_j e^{-D_j/\epsilon}} \leq C_j' e^{-D_j'/\epsilon}. \qquad \square$$

Our next result improves Lemma 3.1 and provides an upper bound on $|\lambda_j^\epsilon(\Omega) - \lambda_j^\epsilon(\Sigma_{\delta^*})|$.

Lemma 3.2. For all $j \in \mathbb{N}$ there exists positive constants C_j and D_j such that

$$|\lambda_j^\epsilon(\Omega) - \lambda_j^\epsilon(\Sigma_{\delta^*})| \leq C_j e^{-D_j/\epsilon}. \tag{27}$$

Proof. The result follows from a proof by contradiction. Let m^* be the first index for which (27) does not hold for any constants $C_j, D_j > 0$, and pick M large and α small. By assumption we can find a sequence $\{\epsilon_k\}$ converging to zero such that

$$|\lambda_{m^*}^{\epsilon_k}(\Omega) - \lambda_{m^*}^{\epsilon_k}(\Sigma_{\delta^*})| > M e^{\frac{-\alpha}{\epsilon_k}}. \tag{28}$$

It then follows from (28) and Proposition C.1 that

$$|\lambda_l^{\epsilon_k}(\Omega) - \lambda_n^{\epsilon_k}(\Sigma_{\delta^*})| > M e^{\frac{-\alpha}{\epsilon_k}} \quad \text{for} \quad n \geq m^* \quad \text{and} \quad l \leq m^*.$$

We recall (26) and apply Proposition C.2 to find that for some positive constants C and D

$$\sum_{j=m*}^{\infty} \langle \chi u_l^{\epsilon_k}(\Omega), u_j^{\epsilon_k}(\Sigma_{\delta^*}) \rangle_{L^2(\Sigma_{\delta^*}, w)}^2 \leq C e^{-D/\epsilon_k} \quad \text{for all} \quad l \leq m^*. \tag{29}$$

Estimates (29) and (25) imply that $\{\chi u_1^{\epsilon_k}(\Omega), ..., \chi u_{m*}^{\epsilon_k}(\Omega)\}$ are approximately linear combinations of $\{u_1^{\epsilon_k}(\Sigma_{\delta^*}), ..., u_{m*-1}^{\epsilon_k}(\Sigma_{\delta^*})\}$. Next, we show that the functions $\{\chi u_1^{\epsilon_k}(\Omega), ..., \chi u_{m*}^{\epsilon_k}(\Omega)\}$ are approximately orthogonal with respect to $\langle \cdot, \cdot \rangle_{L^2(\Sigma_{\delta^*}, w)}$:

$$\left| \langle \chi u_j^{\epsilon_k}(\Omega), \chi u_l^{\epsilon_k}(\Omega) \rangle_{L^2(\Sigma_{\delta^*}, w)} \right| \leq \delta_{jl} + C e^{-D/\epsilon_k} \quad \text{for} \quad j, l \leq m^*. \tag{30}$$

In order to show this, note that Proposition C.4 implies that

$$\langle (1 - \chi) u_j^{\epsilon_k}(\Omega), (1 - \chi) u_j^{\epsilon_k}(\Omega) \rangle_{L^2(\Omega, w)} \leq C e^{-D/\epsilon_k} \quad \text{for} \quad j \leq m^* \tag{31}$$

and so it follows from the Cauchy-Schwartz inequality that

$$\left|\langle(1-\chi)u_j^{\epsilon_k}(\Omega), \chi u_l^{\epsilon_k}(\Omega)\rangle_{L^2(\Omega,w)}\right| \leq Ce^{-D/\epsilon_k} \quad \text{for} \quad j,l \leq m^*. \tag{32}$$

Estimate (30) follows from (31), (32), and the orthonormality of the $\{u_j^\epsilon(\Omega)\}$ with respect to $\langle\cdot,\cdot\rangle_{L^2(\Omega,w)}$.

We now use (26), (29), and (30) to derive a contradiction. For $1 \leq j \leq m^*$ define the vector $u_j^\epsilon \in \mathbb{R}^{m^*-1}$ according to

$$u_j^\epsilon = (\langle\chi u_j^\epsilon(\Omega), u_1^\epsilon(\Sigma_{\delta^*})\rangle_{L^2(\Sigma_{\delta^*},w)}, ..., \langle\chi u_j^\epsilon(\Omega), u_{m^*-1}^\epsilon(\Sigma_{\delta^*})\rangle_{L^2(\Sigma_{\delta^*},w)}).$$

Let $\langle\cdot,\cdot\rangle$ denote the Euclidean inner product on $\mathbb{R}^{m^*-1}$. It follows from (25), (29), and (30) that for any $\delta > 0$, we can find k_0 so that $k > k_0$ implies that

$$\left|\langle u_j^{\epsilon_k}, u_l^{\epsilon_k}\rangle\right| \leq \delta_{jl} + \delta \quad \text{and} \quad \left|\langle u_j^{\epsilon_k}, u_j^{\epsilon_k}\rangle\right| \geq 1-\delta \quad \text{for} \quad 1 \leq j,l \leq m^*. \tag{33}$$

Since we have m^* vectors, $\{u_j^{\epsilon_k}\}_{j=1}^{m^*}$, which belong to $\mathbb{R}^{m^*-1}$, the vectors are linearly dependent. We write

$$u_{m^*}^{\epsilon_k} = c_1^{\epsilon_k}u_1 + ... + c_{m-1}^{\epsilon_k}u_{m^*-1}$$

and note that (33) implies that

$$1 \geq \langle u_{m^*}^{\epsilon_k}, u_{m^*}^{\epsilon_k}\rangle = \langle \sum_{i=1}^{m^*-1} c_i^{\epsilon_k}u_i^{\epsilon_k}, \sum_{i=1}^{m^*-1} c_i^{\epsilon_k}u_i^{\epsilon_k}\rangle$$

$$= \sum_{i,j=1}^{m^*-1} c_i^{\epsilon_k}c_j^{\epsilon_k}\langle u_i^{\epsilon_k}, u_j^{\epsilon_k}\rangle \geq (1-\delta)\sum_{i=1}^{m^*-1}(c_i^{\epsilon_k})^2 - (m^*-1)(m^*-2)(\delta)$$

from which it follows that

$$\sum_{i=1}^{m^*-1}(c_i^{\epsilon_k})^2 \leq \frac{1+(m^*-1)(m^*-2)(\delta)}{1-\delta} \leq K$$

for some fixed constant K. This implies that for $k > k_0$

$$\langle u_{m^*}^{\epsilon_k}, u_{m^*}^{\epsilon_k}\rangle = \langle u_{m^*}^{\epsilon_k}, \sum_{i=1}^{m^*-1} c_i^{\epsilon_k}u_i^{\epsilon_k}\rangle \leq (m^*-1)\delta\sqrt{K}$$

which contradicts (33) if δ is chosen sufficiently small. □

Lemmas 3.1 and 3.2 relate the eigenvalues of (23) to those of (6). Our final lemma, which completes the proof of Theorem 3.1, describes the behavior of the eigenvalues of (6) as $\epsilon \to 0$.

Lemma 3.3. For each $j \in \mathbb{N}$ there exists positive constants C_j and D_j such that

$$|\lambda_j^\epsilon(\Sigma_{\delta^*}) - (\frac{1}{\epsilon} + \lambda_j^\Sigma)| \leq C_j e^{-D_j/\epsilon}. \tag{34}$$

Proof. Let $\{\lambda_\epsilon^j\}_{j=1}^\infty$ be the the eigenvalues of the one dimensional problem

$$-y''(x) + \frac{1}{\epsilon^2}x^2 y(x) - \lambda y(x) = 0 \ \text{ for all } \ x \in (-\delta^*, \delta^*) \ \text{ and } \ y(-\delta^*) = y(\delta^*) = 0. \tag{35}$$

In order to prove Lemma 3.3 it suffices, by Theorem 2.1, to show that for $j = 1, 2$

$$\left|\lambda_\epsilon^j - \frac{2j-1}{\epsilon}\right| \leq C_j e^{-D_j/\epsilon}. \tag{36}$$

We will in fact outline how to establish (36) for all $j \in \mathbb{N}$. The proof of (36) follows from a comparison of the eigenvalues of (35) and those of

$$-y''(x) + \frac{1}{\epsilon^2}x^2 y(x) - \lambda y(x) = 0 \ \text{ for all } \ x \in (-\infty, \infty). \tag{37}$$

Recall that the eigenvalues of (37) are $\left\{\frac{2j+1}{\epsilon}\right\}_{j=0}^\infty$, which correspond to normalized eigenfunctions $\left\{\sqrt{\epsilon}\ h_j\left(\frac{x}{\sqrt{\epsilon}}\right)\right\}_{j=0}^\infty$ [9]. The functions $\{h_j\}_{j=0}^\infty$ are the Hermite functions [9] and can be written as

$$h_j(x) = p_j(x)e^{-\frac{x^2}{2}} \tag{38}$$

where p_j is a polynomial of degree j. These functions form an orthonormal basis for $L^2(\mathbb{R})$ and satisfy

$$-h_j''(x) + x^2 h_j(x) - (2j+1)h_j(x) = 0 \ \text{ for all } \ x \in (-\infty, \infty).$$

Let S_ϵ denote the set of eigenvalues of (35). Our first step towards proving (36) is to show that for all $j \in \mathbb{N}$

$$\text{dist}\left(\frac{2j-1}{\epsilon}, S_\epsilon\right) \leq C_j e^{\frac{-D_j}{\epsilon}} \tag{39}$$

for some positive constants C_j and D_j. Due to the rapid decay of the $\sqrt{\epsilon}\ h_j\left(\frac{x}{\sqrt{\epsilon}}\right)$ away from the origin, (39) follows just as in the proof of Lemma 3.1. We may then prove (36) in the same manner as Lemma 3.2. □

4 Finite element implementation

In Section 3 we proved Theorem 3.1, which relates the eigenvalues of (23) for a bounded domain $\Omega \supset \Sigma$ to those of (1). In practice, we solve the regularized weak eigenvalue problem discussed in Remark 2.1. The regularized problem is solved using the finite element method, chosen because of its well-known convergence estimates for elliptic eigenvalue problems. For completeness, we include one such result here.

Theorem 4.1. ([19], p.230) Let L be a second order elliptic operator with smooth coefficients and let our finite element space F be of degree $(k-1)$. If we denote the eigenvalues of L by $\{\lambda_l\}$ and the approximate eigenvalues by $\{\lambda_\lambda^h\}$, where h is the mesh size, then there is a constant δ such that

$$\lambda_l \leq \lambda_l^h \leq \lambda_l + 2\delta h^{2(k-1)}(\lambda_l)^k$$

We now outline the main steps of our approach, and then discuss each in detail.

Overview of numerical method.

1. Choose mesh and finite dimensional subspace $W(\Omega)_h$.
2. Compute ϕ.
3. Construct the stiffness and load matrices, S and I.

$$S = (S_{ij}) \quad \text{where} \quad S_{ij} = a(u_i, u_j)_\Omega$$

and

$$I = (I_{ij}) \quad \text{where} \quad I_{ij} = (u_i, u_j)_\Omega$$

where $\{u_k\}$ is a basis for $W(\Omega)_h$ and $(\cdot,\cdot)_\Omega$, $a(\cdot,\cdot)_\Omega$ are the regularized bilinear forms discussed at the end of Section 2.2.

4. Solve $Sx = \lambda Ix$.
5. Use the output of the step 4 to solve (1).

Details of numerical method.

1. Throughout the examples in the section 5, Ω is a square (2-D) or cube (3-D), and we use the Cartesian grid with spacing h as our mesh. Our space of finite elements, $W(\Omega)_h$, is given, for general space dimension n, by

$$W(\Omega)_h = \{f : \Omega \to \mathbb{R} : f \in C(\bar{\Omega}) \text{ and n-linear on each cube with side length } h\}.$$

Theorem 4.1 suggests that second order accuracy is possible.

2. As suggested by Theorem 3.1, the signed distance function used in computations only needs to be accurate near Σ. Such a function can be found, for example, as the solution of

$$\phi_t + \text{sgn}(\phi)(|\nabla\phi| - 1) = 0 \tag{40}$$

with initial data of the form

$$\phi(x,0) = \begin{cases} < 0 & \text{if } x \text{ is inside } \Sigma \\ > 0 & \text{if } x \text{ is outside } \Sigma \end{cases}$$

after a short amount of time. This follows from the method of characteristics. We solve (40) using second order ENO [15].

3. Recall from example 2.2 that in order to compute $a(\cdot,\cdot)_\Omega$, the function $a : \Sigma \to \mathbb{R}$ needs to be extended to a function defined on Ω which satisfies (22) near Σ. We take our extension to be the solution of

$$\frac{\partial u}{\partial t} + \text{sign}(\phi)\langle\nabla u, \nabla\phi\rangle = 0 \quad x \in \Omega \tag{41}$$

$$u(\cdot, t = 0) \text{ is an arbitrary extension of } a.$$

after a short amount of time. This method was introduced in [5].

Computing $(\cdot,\cdot)_\Omega$ and $a(\cdot,\cdot)_\Omega$ requires computing integrals over Ω. We compute these integrals over each cube with side length h using the trapezoidal rule. Since one needs to know the value of ϕ and its derivatives at each point used in the integration, we felt this choice of integration scheme was a good compromise between accuracy and efficiency. All relevant geometric quantities are computed using standard finite differences on the Cartesian grid.

4. We solve $Sx = \lambda Ix$ using Matlab's eigs routine. The eigs routine can calculate the first five eigenvalues of a sparse $45,000 \times 45,000$ matrix in a few minutes on a desktop PC.

5. The final step is to calculate the eigenvalues of (1) from those computed in the previous step, $\{\lambda_i^{\text{computed}}\}$. Let $\widetilde{\lambda_i^\Sigma}$ refer to our numerical approximation of λ_i^Σ; in light of Theorem 3.1, it is reasonable to set

$$\widetilde{\lambda_i^\Sigma} = \lambda_i^{\text{computed}} - \frac{1}{\epsilon} \tag{42}$$

for small i. In practice, this approximation performs poorly. A general rule for eigenvalue calculations, supported by Theorem 4.1, is that larger (in magnitude) eigenvalues are more difficult to compute than smaller ones. It appears that part of the reason for the poor performance of the approximation (42) is the size of the $\{\lambda_i^{\text{computed}}\}$, each of which is of the order of $\frac{1}{\epsilon}$, where $\epsilon << 1$.

One simple solution to this is to rescale the coefficients of L in order to reduce the size of the $\{\lambda_i^{\text{computed}}\}$. We achieve this by setting

$$L^\nu = L_\Sigma - (\epsilon)^\nu \langle D^2 u(x) \nabla\phi(x), \nabla\phi(x)\rangle + \frac{1}{\epsilon^{2-\nu}} \cdot (\phi(x))^2 u^2(x), \tag{43}$$

where $0 < \nu < 1$, and solving the weak eigenvalue problem for L^ν. Since the eigenvalues of L^ν are roughly $\{\frac{2n-1}{\epsilon^{1-\nu}} + \lambda_m^\Sigma\}_{m,n=1}^\infty$, it is reasonable to set

$$\widetilde{\lambda_i^\Sigma} = \lambda_i^{\text{computed}} - \frac{1}{\epsilon^{1-\nu}} \tag{44}$$

for small i. However, we achieved much better results using the approximation

$$\widetilde{\lambda_i^\Sigma} = \lambda_i^{\text{computed}} - \lambda_1^{\text{computed}}. \tag{45}$$

We do not have an entirely satisfactory explanation for the improvement of (45) over (44). By Theorems 2.1 and 3.1, we may decompose $\lambda_i^{\text{computed}}$ into radial and surface components, which we write as

$$\lambda_i^{\text{computed}} \approx \lambda_i^\Sigma + \lambda_i^{\text{computed},r},$$

where $\lambda_i^{\text{computed},r} \approx \frac{1}{\epsilon^{1-\nu}}$. Using this terminology, the drastic improvement of (45) over (44) is due to

$$\left|\lambda_i^{\text{computed},r} - \lambda_1^{\text{computed},r}\right| << \left|\frac{1}{\epsilon^{1-\nu}} - \lambda_i^{\text{computed},r}\right|.$$

Choosing ν in (43) is a compromise. As ν increases, the eigenvalues of L^ν decrease, which translates to quicker convergence. However, ν needs to be chosen small enough to ensure that the initial eigenvalues of L^ν are approximately

$$\frac{1}{\epsilon^{1-\nu}}, \frac{1}{\epsilon^{1-\nu}} + \lambda_2^\Sigma, \frac{1}{\epsilon^{1-\nu}} + \lambda_3^\Sigma, ... \tag{46}$$

In order to chose ν effectively, one needs to have a good estimate of the magnitude of the λ_i^Σ that one is interested in computing. One way to get such an estimate is to choose ϵ very small and $\nu = 0$.

5 Numerical results

In this section, we examine the results of computations carried out using the method discussed in Section 4. We use (45) to approximate the $\left\{\lambda_i^\Sigma\right\}$ from the $\{\lambda_i^{\text{computed}}\}$.

5.1 Examples and results

Laplacian on the unit circle. For our first example, $\Sigma = S^1$, $a \equiv 1$, $\nu = .6$, and $\Omega = [-1.5, 1.5]^2$. See Figures 1 and 2 for pictures of the eigenfunctions and Table 1 for error analysis.

Laplacian on an ellipse. Our next example is the ellipse

$$\Sigma = \left\{(x, y) : \left(\frac{x}{0.8}\right)^2 + \left(\frac{y}{0.4}\right)^2 = 1\right\}$$

with $a(x) \equiv 1$ and $\Omega = [-1, 1]^2$. We set $\nu = .6$. See Figures 3 and 4 for pictures of the eigenfunctions and Table 2 for error analysis.

Piecewise constant $a(x)$ on the unit circle. In this example $\Sigma = S^1$,

$$a(x, y) = \begin{cases} 1 & \text{if } y > 0 \\ 2 & \text{if } y < 0 \end{cases}$$

and $\Omega = [-1.5, 1.5]^2$. Again, we set $\nu = .6$. See Figures 5 and 6 for pictures of the eigenfunctions and Table 3 for error analysis.

Laplacian on two circles. Here we consider the case of the Laplacian on

$$\Sigma = \{(x, y) : (x - .75)^2 + y^2 = .3^2\} \cup \{(x, y) : (x + .75)^2 + y^2 = .3^2\}$$

and set $\nu = .6$. See Figures 7 and 8 for pictures of the eigenfunctions and Table 4 for error analysis. Note that our method captures the multiplicity of the eigenvalues

Laplacian on a flower. We now consider the case of a more challenging curve, given in polar coordinates by

$$\mathrm{r}(\theta) = 2\cos^2(\theta)\sin^2(\theta) + .3 \quad \text{(see Figure 9)}.$$

We set $a \equiv 1$ and $\Omega = [-1, 1]^2$. For $\epsilon = 1/100$ and $1/200$, we set $\nu = .6$; for $\epsilon = 1/400$ we set $\nu = .8$. See Figures 10 and 11 for pictures of the eigenfunctions and Table 5 for error analysis. It appears that ϵ needs to be chosen quite small in this example due to the flower's cusps.

Laplacian on the unit sphere. Now we consider the simplest three dimensional case, $\Sigma = S^2$ and $a \equiv 1$. We set $\nu = .8$. See Table 6 for results.

Laplacian on the union of two unit spheres. We now consider the more complicated case

$$\Sigma = \{(x, y, z) : (x - 1.5)^2 + y^2 + z^2 = 1\} \cup \{(x, y, z) : (x + 1.5)^2 + y^2 + z^2 = 1\}$$

with $a \equiv 1$ and $\nu = .8$. See Table 7 for results.

Table 1: Laplacian on the unit circle.

$\frac{1}{\epsilon}$	dx	% relative error λ_1^Σ	% relative error λ_2^Σ	% relative error λ_3^Σ	% relative error λ_4^Σ
100	.075	1.06	1.06	3.22	5.87
	.0375	0.33	0.33	1.15	1.74
	.025	0.15	0.15	0.47	0.80
	.01875	0.09	0.09	0.27	0.45
	.015	0.06	0.06	0.19	0.31
	.0125	0.04	0.05	0.14	0.22
200	.075	0.63	0.63	11.35	16.68
	.0375	0.44	0.44	4.28	5.70
	.025	0.25	0.25	2.14	2.77
	.01875	0.15	0.15	1.27	1.63
	.015	0.10	0.10	0.86	1.06
	.0125	0.07	0.07	0.60	0.76

Table 2: Laplacian on an ellipse.

$\frac{1}{\epsilon}$	dx	% relative error λ_1^Σ	% relative error λ_2^Σ	% relative error λ_3^Σ	% relative error λ_4^Σ
100	.05	8.00	11.89	0.71	2.31
	.025	3.20	4.97	0.37	1.16
	.0167	1.96	3.42	0.30	0.94
	.0125	1.53	2.79	0.32	0.81
	.01	1.27	2.45	0.32	0.74
200	.05	9.89	15.21	2.10	2.70
	.025	2.55	4.66	0.92	1.17
	.0167	0.92	2.50	0.74	0.85
	.0125	0.33	1.65	0.64	0.68
	.01	0.50	1.25	0.59	0.61

Table 3: Piecewise constant $a(x)$ on the unit circle.

$\frac{1}{\epsilon}$	dx	% relative error λ_1^Σ	% relative error λ_2^Σ	% relative error λ_3^Σ	% relative error λ_4^Σ
100	.0625	0.87	0.27	3.77	1.56
	.0313	0.23	0.21	1.31	0.17
	.0206	0.31	0.32	0.80	0.21
	.0156	0.38	0.38	0.61	0.37
	.0125	2.03	1.03	1.90	0.75
	.0104	0.29	0.33	0.89	0.07
200	.0625	6.92	2.36	4.08	0.64
	.0313	0.50	0.07	3.75	2.34
	.0206	0.77	0.07	2.03	0.10
	.0156	0.14	0.16	1.38	0.40
	.0125	1.96	1.18	2.56	1.27
	.0104	0.29	0.33	0.89	0.07

Table 4: Laplacian on the union of two circles.

$\frac{1}{\epsilon}$	dx	% relative error λ_1^Σ	% relative error λ_2^Σ	% relative error λ_3^Σ
100	.075	1.65	1.65	1.65
	.0375	0.34	0.34	0.34
	.025	0.18	0.18	0.18
	.0187	0.12	0.12	0.12
	.015	0.09	0.09	0.09
	.0125	0.08	0.08	0.08
200	.075	1.84	1.84	1.84
	.0375	0.58	0.58	0.58
	.025	0.28	0.28	0.28
	.0187	0.16	0.16	0.16
	.015	0.11	0.11	0.11
	.0125	0.07	0.07	0.07

Table 5: Laplacian on a flower.

$\frac{1}{\epsilon}$	dx	% relative error λ_1^Σ	% relative error λ_2^Σ	% relative error λ_3^Σ	% relative error λ_4^Σ
100	.05	11.35	11.35	8.41	14.09
	.025	7.81	7.81	6.37	7.71
	.0167	6.86	6.93	3.94	8.00
	.0125	6.66	6.66	2.93	8.55
	.01	6.30	6.30	2.27	9.04
200	.05	10.77	10.77	9.78	12.10
	.025	5.33	5.33	3.65	7.01
	.0167	3.81	3.81	0.84	6.81
	.0125	3.35	3.35	0.31	7.09
	.01	3.15	3.15	0.91	7.34
400	.05	11.02	11.02	7.30	14.95
	.025	4.81	4.81	2.74	6.84
	.0167	3.03	3.03	2.22	3.73
	.0125	2.47	2.47	1.90	3.00
	.01	2.09	2.09	1.60	2.47

Table 6: Laplacian on the unit sphere.

$\frac{1}{\epsilon}$	dx	% relative error λ_1^Σ	% relative error λ_2^Σ	% relative error λ_3^Σ
100	.25	5.21	5.21	5.21
	.167	3.13	3.13	3.13
	.125	2.08	2.08	2.08
	.1	1.49	1.49	1.49
200	.25	6.35	6.35	6.35
	.167	4.07	4.07	4.07
	.125	2.78	2.78	2.78
	.1	2.04	2.04	2.04

Table 7: Laplacian on the union of two unit spheres.

$\frac{1}{\epsilon}$	dx	% relative error λ_1^Σ	% relative error λ_2^Σ	% relative error λ_3^Σ
100	.25	77.35	75.00	123.00
	.167	5.13	5.21	5.37
	.125	6.40	6.48	6.50
	.1	2.32	2.49	6.43
200	.25	62.00	53.00	207.00
	.167	2.30	2.30	2.00
	.125	7.23	7.32	7.36
	.1	6.23	5.93	13.93

5.2 Discussion of results

Due to the steep gradients of the eigenfunctions of the domain problem near Σ, our method, in its current form, is ineffective for 3-D calculations. In order to remedy this, we need to develop numerical methods which are better able to resolve the steep gradients of the eigenfunctions of (7). A natural approach would be to use a non-uniform mesh, fine near Σ and rough far from Σ, to solve (7). Such a mesh was used in [3] for solving elliptic PDE on surfaces. Figures 13 and 14 demonstrate the poor resolution which results from an insufficiently fine mesh near Σ.

6 Conclusion and future work

In this paper, we have shown how the eigenvalues of (1) can be found by solving a regularized version of the elliptic eigenvalue problem (7) in a domain containing the surface Σ. The main results used to justify this approach are Theorem 2.1, which follows from a standard separation of variables argument, and Theorem 3.1, the proof of which relies on estimates from the semiclassical analysis of the Schrödinger operator.

One challenge for the future is solving elliptic PDE, including eigenvalue problems, on hypersurfaces with boundary. We describe here one approach, which combines ideas from this paper with the fictitious domain method, to handle Dirichlet or Neumann boundary

conditions. In order to solve (1) with Dirichlet boundary conditions, we first extend Σ to a closed surface $\tilde{\Sigma}$, and then solve

$$-\nabla_S \cdot (\tilde{a}(x)\nabla_S u) + V(x)u = \lambda u$$

on $\tilde{\Sigma}$ using the method discussed in Section 4. Here, $\tilde{a} : \tilde{\Sigma} \to \mathbb{R}$ is an extension of $a : \Sigma \to \mathbb{R}$ and the potential V satisfies

$$V(x) = 0 \text{ if } x \in \Sigma \text{ and } V(x) = \mathrm{C} \quad \text{for} \quad x \in \tilde{\Sigma} \setminus \Sigma \quad \text{where} \quad C >> 1.$$

In order to solve (1) with Neumann boundary conditions, we propose solving

$$-\nabla_S \cdot (\tilde{a}(x)\nabla_S u) = \lambda u \quad \text{for } x \in \tilde{\Sigma}$$

where $\tilde{a}$ is an extension of a which satisfies

$$\tilde{a}(x) = \delta << 1 \quad \text{for } x \in \tilde{\Sigma} \setminus \Sigma.$$

7 Acknowledgements

The author would like to thank Professor Stanley Osher for his support and guidance while working on this problem, and Professor James Ralston for his suggestion of introducing a single-well potential and, more generally, the approach taken in Section 3. The author would also like to thank Professor Chris Anderson for suggesting the finite element implementation and Ernie Esser and Xinwei Zhang for valuable conversations.

This material is based upon work supported under a National Science Foundation Graduate Research Fellowship.

A Solving parabolic equations on surfaces

In [11], Greer proposed a method for solving parabolic equations on surfaces using finite differences which improved on the approach of [2]. In order to solve

$$u_t = \nabla_S \cdot (a\nabla_S u) \tag{47}$$

on Σ, Greer's method solves

$$u_t = -L_\Sigma u + \epsilon\langle D^2 u \nabla\phi, \nabla\phi\rangle \tag{48}$$

in a domain Ω containing Σ using finite differences. We now prove Greer's main result, which justifies his approach, for linear PDE of the form (47). The proof uses Proposition 2.1 and the completeness of the eigenfunctions of $-\nabla_S \cdot a\nabla_S$ in $H^1(\Sigma)$. We first state the result.

Theorem A.1. [11] Let $\Omega = \Sigma_\delta$ for δ small enough so that (9) holds. Let $u \in C^2(\mathbb{R}^n \times [0,T])$ be a solution to

$$u_t = -L_\Sigma u + c(x)\langle D^2 u \nabla\phi, \nabla\phi\rangle \quad \text{with initial data} \quad u(\cdot, t=0) = g(\cdot). \tag{49}$$

Here, $c \geq c_1 > 0$, for some constant c_1. If g is constant in the normal direction, i.e. $\langle \nabla g, \nabla\phi\rangle \equiv 0$, then $\langle \nabla u, \nabla\phi\rangle \equiv 0$ for all time $t > 0$.

We learned about Greer's work only after establishing the results in Section 2 and Appendix B. Greer's result holds for more general PDE than those discussed here, including certain nonlinear PDE.

Earlier methods for solving (47) based on implicit surfaces did not possess the orthogonality property described in Theorem A.1 [2]. As a result, solutions obtained from these methods develop variation in the normal direction, which can lead to numerical error when computing ∇_S and $\nabla_S \cdot$. One technique for minimizing this variation is to frequently re-initialize solutions off of Σ to be constant along normals to Σ [12, 21]; an advantage of Greer's method is that in practice it requires fewer re-initializations. See [11] for more on this and other advantages of Greer's method.

Proof of Theorem A.1. By uniqueness, it suffices to find a solution to (49) which remains constant in the normal direction. Because of the completeness of the eigenfunctions of $-\nabla_S \cdot a \nabla_S$ and (9) we can decompose any smooth function $u : \Sigma_\delta \to \mathbb{R}$ as

$$u(x,t) = \sum_{n=0}^{\infty} f_n(x - \phi(x)\nabla\phi(x)) k_n(\phi(x), t).$$

Here, the $\{f_n\}$ are eigenfunctions of $-\nabla_S a \cdot \nabla_S$, with eigenvalues $\{\lambda_n^\Sigma\}$, which form an orthonormal basis for $L^2(\Sigma)$, and each $k_n : [-\delta, \delta] \times [0, \infty) \to \mathbb{R}$ is a smooth function. Because of our hypothesis on the initial data, we have that

$$u(x, t = 0) = \sum_{n=0}^{\infty} f_n(x - \phi(x)\nabla\phi(x)) g_n$$

where the $\{g_n\}$ are constants. Separating variables as in the proof of Proposition 2.1, we have that

$$u(x,t) = \sum_{n=0}^{\infty} f_n(x - \phi(x)\nabla\phi(x)) g_n e^{-\lambda_n^\Sigma t}$$

solves (49). □

B Computing L

In this appendix, we provide formulas for L, valid in domains Ω in which (9) holds, which demonstrate that L can be written in divergence form. Ellipticity of L follows from these results. Proposition B.1 expresses L_Σ and L_n in terms of the differential operators $\frac{\partial}{\partial x_i}$, where $\{x_i\}$ is the standard basis for $\mathbb{R}^n$, while Proposition B.2 expresses L_Σ in terms of the operators $\frac{\partial}{\partial e_i}$, where $\{e_i(x)\}$ represent the directions of principal curvature of the $\phi(x)$ level-set at x. We work in three space dimensions in Proposition B.1 for simplicity, and assume throughout this section that a, originally defined only on Σ, is defined in all of Ω according to (22).

Proposition B.1. Let $\Omega \subset \mathbb{R}^3$ be a domain such that (9) holds and let $u \in C^2(\Omega)$. Then for all $x \in \Omega$,

$$L_\Sigma u = -w(x) \sum_{i,j=1}^{3} \left[\left(\frac{1 - \phi(x)\kappa_2(x)}{1 - \phi(x)\kappa_1(x)} \langle x_i, e_1 \rangle \langle x_j, e_1 \rangle + \frac{1 - \phi(x)\kappa_1(x)}{1 - \phi(x)\kappa_2(x)} \langle x_i, e_2 \rangle \langle x_j, e_2 \rangle \right) a(x) u_{x_i} \right]_{x_j}$$

and

$$L_n u = -w(x) \sum_{i,j=1}^{3} \left[\left(\frac{1}{w(x)} \langle x_i, \nabla\phi(x)\rangle \langle x_j, \nabla\phi(x)\rangle u_{x_i} \right) \right]_{x_j}$$

where $w(x) = \frac{1}{(1-\phi(x)\kappa_1(x))(1-\phi(x)\kappa_2(x))}$ and $\{x_i\}$ is the standard basis for $\mathbb{R}^n$.

Proof. The proof follows from integration by parts and an application of the geometric identities discussed in Section 2.2. We first consider the identity for L_Σ. Let $v \in C_c^2(\Omega)$; from (15) we have

$$(L_\Sigma u, v)_\Omega = \int_\Omega (1-\phi(x)\kappa_1(x))(1-\phi(x)\kappa_2(x)) L_\Sigma(u) \cdot v \; dx. \tag{50}$$

On the other hand, by (20), (11), and (19), we have that $(L_\Sigma u, v)_\Omega$ equals

$$\int_\Omega a(x) \frac{1-\phi(x)\kappa_2(x)}{1-\phi(x)\kappa_1(x)} \langle \nabla u(x), e_1\rangle \langle \nabla v(x), e_1\rangle + a(x) \frac{1-\phi(x)\kappa_1(x)}{1-\phi(x)\kappa_2(x)} \langle \nabla u(x), e_2\rangle \langle \nabla v(x), e_2\rangle \; dx$$

$$= \int_\Omega a(x) \sum_{i,j=1}^{3} \left[\frac{1-\phi(x)\kappa_2(x)}{1-\phi(x)\kappa_1(x)} \langle x_i, e_1\rangle \langle x_j, e_1\rangle + \frac{1-\phi(x)\kappa_1(x)}{1-\phi(x)\kappa_2(x)} \langle x_i, e_2\rangle \langle x_j, e_2\rangle \right] u_{x_i} v_{x_j} \; dx.$$

Integrating the above expression by parts we find that $(L_\Sigma u, v)_\Omega$ equals

$$\int_\Omega - \sum_{i,j=1}^{3} \left[\left(\frac{1-\phi(x)\kappa_2(x)}{1-\phi(x)\kappa_1(x)} \langle x_i, e_1\rangle \langle x_j, e_1\rangle + \frac{1-\phi(x)\kappa_1(x)}{1-\phi(x)\kappa_2(x)} \langle x_i, e_2\rangle \langle x_j, e_2\rangle \right) a(x) u_{x_i} \right]_{x_j} v \; dx$$

Setting the above equation equal to (50) and noting that $v \in C_c^2(\Omega)$ is arbitrary, the result follows.

The identity for L_n follows a similar approach. First note that by (15) we have

$$(L_n u, v)_\Omega = \int_\Omega \frac{1}{w(x)} L_n u \cdot v \; dx. \tag{51}$$

Next, note that (9) and integration by parts yield

$$(L_n u, v)_\Omega = \int_\Omega \frac{1}{w(x)} \langle \nabla u(x), \nabla\phi(x)\rangle \langle \nabla v(x), \nabla\phi(x)\rangle \; dx$$

$$= -\int_\Omega \sum_{i,j=1}^{3} \left[\left(\frac{1}{w(x)} \langle x_i, \nabla\phi(x)\rangle \langle x_j, \nabla\phi(x)\rangle u_{x_i} \right) \right]_{x_j} v \; dx. \tag{52}$$

The identity for L_n follows by equating (51) and (52). □

The next proposition expresses L_Σ in terms of the differential operators $\frac{\partial}{\partial e_i}$.

Proposition B.2. Let $\Omega \subset \mathbb{R}^n$ be a domain such that (9) holds and let $u \in C^2(\Omega)$. Then for all $x \in \Omega$,

$$L_\Sigma u|_x = \sum_{i=1}^{n-1} \frac{1}{1-\phi(x)\kappa_i(x)} \frac{\partial}{\partial e_i} \left(\frac{a(x)}{1-\phi(x)\kappa_i(x)} \frac{\partial}{\partial e_i} u \right).$$

Proof. First note that (11) and (19) imply

$$(\nabla_S^r u)(s) = \sum_{i=1}^{n-1} \frac{1}{1 - r\kappa_i(s + r\nabla\phi(s))} \left(\frac{\partial}{\partial e_i} u|_{s+r\nabla\phi(s)} \right) e_i. \tag{53}$$

Next, note that if $g \in C^1(\Omega)$, $f = g^{\phi(x)}$, and e is a direction of principal curvature at x, then by the chain rule and (19)

$$\frac{\partial}{\partial e} f|_{x-\phi(x)\nabla\phi(x)} = \langle \nabla g|_x, [I + \phi(x) D^2\phi|_{x-\phi(x)\nabla\phi(x)}]e \rangle = \frac{1}{1 - \phi(x)\kappa(x)} \frac{\partial}{\partial e} g|_x.$$

The proposition follows from (53) by setting $g(x) = \frac{a(x)}{1-\phi(x)\kappa_i(x)} \frac{\partial}{\partial e_i} u$ in the above formula. □

Corollary B.1. Let $\Omega \subset \mathbb{R}^n$ be a domain such that (9) holds. Then L is elliptic in Ω.

Proof. The result follows immediately from Proposition B.1, since $\{e_1, e_2, \nabla\phi\}$ form an orthonormal basis and $1 - \phi(x)\kappa_i(x) > 0$. The result also follows from Proposition B.2 by a change of coordinates. □

C Some results from spectral theory

We collect here some well-known results from elliptic PDE, the spectral theory of self-adjoint operators, and the semi-classical analysis of the Schrödinger operator.

Proposition C.1. (Monotonicity of Dirichlet eigenvalues with respect to domain) Let L be a symmetric second-order linear elliptic operator, and let $\{\lambda_n^\Omega\}$ be the eigenvalues of the problem $Lu = \lambda u$ subject to the boundary condition $u = 0$ on $\partial\Omega$. Then for $j = 1, 2, ...$

$$\lambda_j^{\Omega_1} \leq \lambda_j^{\Omega_2} \quad \text{if} \quad \Omega_1 \supset \Omega_2 \tag{54}$$

Proof. The result follows from the min-max formula for the $\{\lambda_l^\Omega\}$ [19]:

$$\lambda_l^\Omega = \inf_{S_l} \sup_{v \in S_l} R(v).$$

Here, $S_l = \{V \subset H_0^1(\Omega) : V \text{ is an l-dimensional subspace of } H_0^1(\Omega)\}$ and $R(v)$, the Rayleigh quotient, is defined as

$$R(v) = \frac{(Lv, v)}{(v, v)}.$$ □

Proposition C.2. (Distance to the spectrum) Let H be a Hilbert space, D a dense subspace of H, and $T : D \to H$ a self-adjoint linear operator. Then for $z \in \text{spec}(T)^c$

$$\|(T - zI)^{-1}\| = \frac{1}{\text{dist}(z, \text{spec}(T))}$$

which implies

$$\text{dist}(z, \text{spec}(T)) \leq \frac{\|(T - zI)u\|}{\|u\|}. \tag{55}$$

Corollary C.1. If $\|u\| \approx 1$ and $\|(T - zI)u\| << 1$, then $\text{dist}(z, \text{spec}(T)) << 1$.

Proof. The result follows directly from Proposition C.2. □

Under the assumption that a linear operator T has a basis of eigenfunctions, Proposition C.3 states that if $\|(T - zI)u\| << 1$ and $\|u\| \approx 1$, then u is nearly a linear combination of those eigenfunctions with eigenvalues near z.

Proposition C.3. Let H be a Hilbert space and $T : H \to H$ a linear operator. Assume that there exists an orthonormal basis $\{f_j\}$ of H consisting of eigenfunctions of T with eigenvalues $\{\lambda_j\}$. Let $u \in H$ and assume $\|(T - zI)u\| < \epsilon$ for some $z \in \mathbb{R}$. Fix $\delta > 0$ and let $I = \{j : |\lambda_j - z| \geq \delta\}$. Then

$$\sum_{j \in I} \langle u, f_n \rangle^2 < \frac{\epsilon^2}{\delta^2}. \tag{56}$$

Proof. The result follows from the Pythagorean theorem:

$$(T - zI)u = \sum_{j=1}^{\infty} (\lambda_j - z)\langle u, f_n \rangle f_n \Rightarrow \sum_{j=1}^{\infty} (\lambda_j - z)^2 \langle u, f_n \rangle^2 = \epsilon^2 \Rightarrow$$

$$\delta^2 \sum_{j \in I} \langle u, f_n \rangle^2 \leq \sum_{j \in I} (\lambda_j - z)^2 \langle u, f_n \rangle^2 < \epsilon^2. \qquad \square$$

Next, we state a result which provides very useful information regarding the behavior of eigenfunctions u_h of

$$-h^2 \Delta u_h + V(x) u_h = \lambda_h u_h \quad \text{for} \quad x \in \Omega \quad \text{and} \quad u_h = 0 \quad \text{on} \quad \partial\Omega \tag{57}$$

as $h \to 0$ [13]. Here, $0 \leq V(x) \in C(\bar{\Omega})$ is a potential. We use a variant of this result in the proof of Theorem 3.1 to describe the behavior of eigenfunctions of (23) as $\epsilon \to 0$. We first make a definition.

Definition C.1. (Agmon distance) The Agmon distance $d(x, y)$ between two points x and y is defined to to be

$$d(x, y) = \inf_{\gamma \in C} \int_{\gamma} \sqrt{V} \, ds$$

where C is the set of all piecewise C^1 curves connecting x and y [13]. If $T \subset \Omega$, we define $d(x, T)$ to be

$$d(x, T) = \inf_{y \in T} d(x, y).$$

Note that the Agmon distance depends on the potential V. We now state a result, Proposition C.4, which provides an estimate of the decay of eigenfunctions of (57) away from $U = \{x \in \Omega : V(x) = \min_{z \in \bar{\Omega}} V(z)\}$ as $h \to 0$.

Proposition C.4. (See Proposition 3.3.1 and Corollary 3.3.2 in [13]) Let $\{u_h\}_{h\in J}$ where $J \subset [0, h_0]$ be a family of eigenfunctions of (57) normalized so that $\|u_h\|_{L^2(\Omega)} = 1$. Assume that $\lambda_h \to 0$ as $h \to 0$. Let $U = \{x \in \Omega : V(x) = \min_{z\in\bar{\Omega}} V(z)\}$. Then for each $\delta > 0$ there exists $C_\delta > 0$ such that for all $h \in J$

$$\left\|\nabla\left(e^{\frac{d(x,U)}{h}}u_h\right)\right\|_{L^2(\Omega)} + \left\|e^{\frac{d(x,U)}{h}}u_h\right\|_{L^2(\Omega)} \leq C_\delta e^{\frac{\delta}{h}}. \tag{58}$$

It follows from (58) that the L^2 norm of u_h is concentrated in U: for each open neighborhood $V \supset U$ we have

$$\|u_h\|_{L^2(V)} = 1 + O\left(e^{\frac{-\delta}{h}}\right). \tag{59}$$

One can check that a variant of Proposition C.4 applies to the eigenvalue problem (23) under the assumptions outlined at the beginning of Section 3. In the context of (23), $h = \epsilon$, $V = \psi$ and $U = \Sigma$.

References

[1] M. Berger, *A Panoramic View of Riemannian Geometery*, Springer-Verlag, Berlin, 2003.

[2] M. Bertalmoio, L.T. Cheng, G. Sapiro, and S. Osher, Variational problems and partial differential equations on implicit surfaces, J. Comp. Phys., 174 (2): 759-780, December 2001.

[3] M. Burger, Finite element approximation of elliptic partial differential equations on implicit surfaces, UCLA CAM Report 05-46, August 2005.

[4] L.T. Cheng, P. Burchard, B. Merriman, and S. Osher, Motion of Curves Constrained on Surfaces Using a Level-Set Approach, Journal of Computational Physics, 175 (2): 604-644, January 2002.

[5] S. Chen, B. Merriman, S. Osher, and P. Smereka, A simple level set method for solving Stefan problems, Journal of Computational Physics, 135 (1): 8-29, July 1997.

[6] R. Courant and D. Hilbert, *Methods of Mathematical Physics Vol. 1*, Interscience, New York, 1970.

[7] L. Evans, *Partial Differential Equations*, American Mathematical Society, United States, 1998.

[8] L. Evans and R. Gariepy, *Measure Theory and Fine Properties of Functions*, CRC Press, Florida, 1992.

[9] G. Folland, *Fourier Analysis and its Applications*, Wadsworth and Brooks, United States, 1992.

[10] D. Gilbarg and N. Trudinger, *Elliptic Partial Differential Equations of Second Order*, Springer-Verlag, Berlin, 2001.

[11] J.B. Greer, An improvement of a recent Eulerian method for solving PDEs on general geometries, Journal of Scientific Computing, 29(3): 321-351, December 2006.

[12] J.B. Greer, A.L. Bertozzi, and G. Sapiro, Fourth order partial differential equations on general geometries, J. Comp. Phys., 216 (1): 216-246, 2006.

[13] B. Helffer, *Semi-Classical Analysis for the Schrödinger Operator and Applications*, Lecture Notes in Mathematics 1336, Springer-Verlag, Germany, 1988.

[14] F. Morgan, *Riemannian Geometry: A Beginner's Guide*, A.K. Peters, Wellesley, 1998.

[15] S. Osher and R. Fedkiw, *Level Set Methods and Dynamic Implicit Surfaces*, Springer-Verlag, New York, 2003.

[16] S. Osher and J.A Sethian, Fronts Propagating with Curvature-Dependent Speed: Algorithms Based on Hamilton–Jacobi Formulations, Journal of Computational Physics, 79: 12-49, 1988.

[17] M. Reuter, F.-E. Wolter, and N.Peinecke, Laplace-Beltrami spectra as 'Shape-DNA' of surfaces and solids, Computer Aided Design, vol. 38, p.342-366, 2006.

[18] S. Rosenberg, *The Laplacian on a Riemannian Manifold: An Introduction to Analysis on Manifolds*, Cambridge University Press, United Kingdom, 1998.

[19] G. Strang and G. Fix, *An Analysis of the Finite Element Method*, Prentice-Hall, Englewood Cliffs, 1973.

[20] N. Trudinger, *Linear Elliptic Operators with Measurable Coefficients*, Ann. Scuola Norm. Sup. Pisa (3), 27, 265-308, 1973.

[21] J. Xu and H.-K. Zhao, An Eulerian formulation for solving partial differential equations along a moving interface, J. Sci. Comput., 19 (1-3): 573-594, 2003. Special issue in honor of the sixtieth birthday of Stanley Osher

[22] W. Ziemer, *Weakly Differentiable Functions*, Springer Verlag, Berlin, 1999.

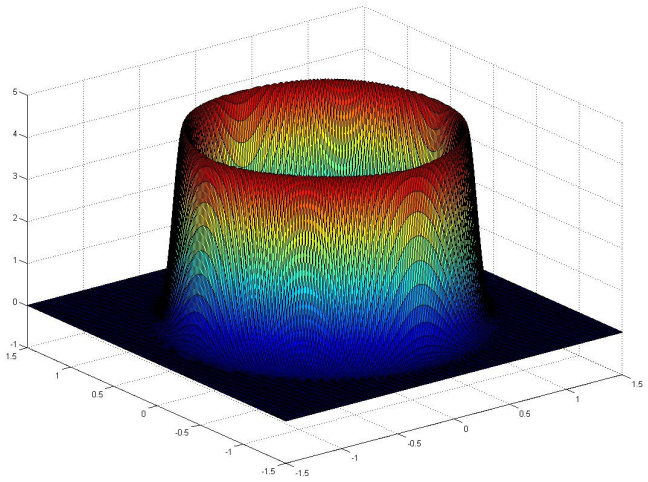

Figure 1: First eigenfunction, $\Sigma = S^1$, $a \equiv 1$, $\frac{1}{\epsilon} = 200$.

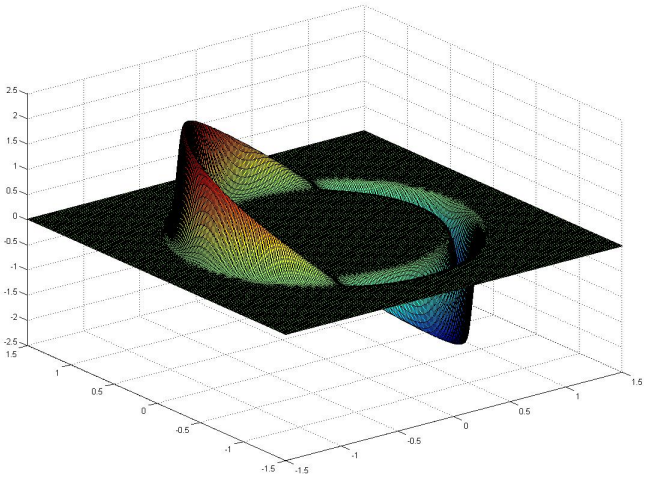

Figure 2: Second eigenfunction, $\Sigma = S^1$, $a \equiv 1$, $\frac{1}{\epsilon} = 500$.

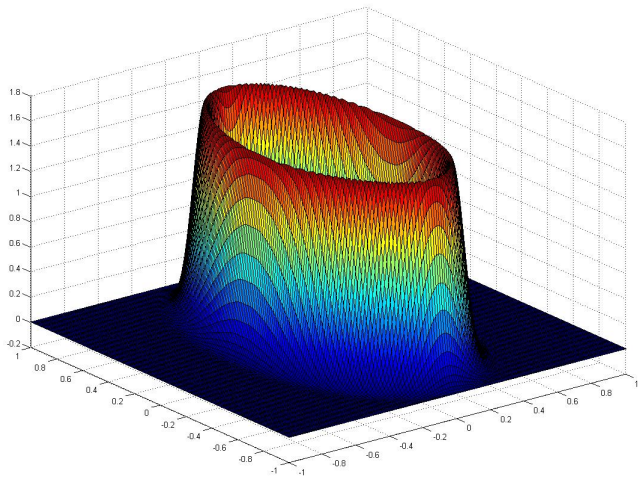

Figure 3: First eigenfunction, $\Sigma =$ ellipse, $a \equiv 1$, $\frac{1}{\epsilon} = 300$.

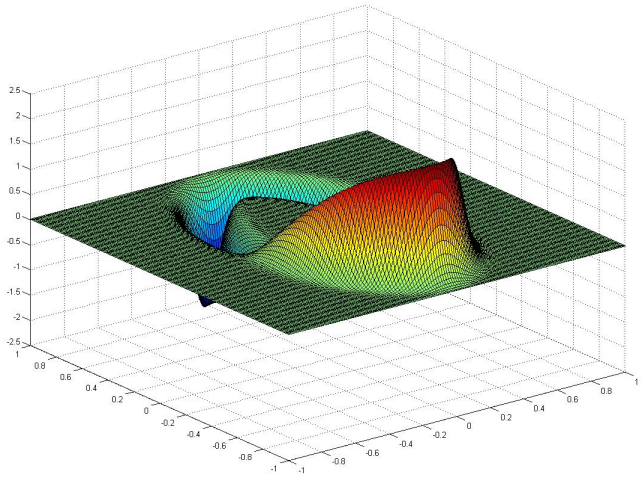

Figure 4: Second eigenfunction, $\Sigma =$ ellipse, $a \equiv 1$, $\frac{1}{\epsilon} = 300$.

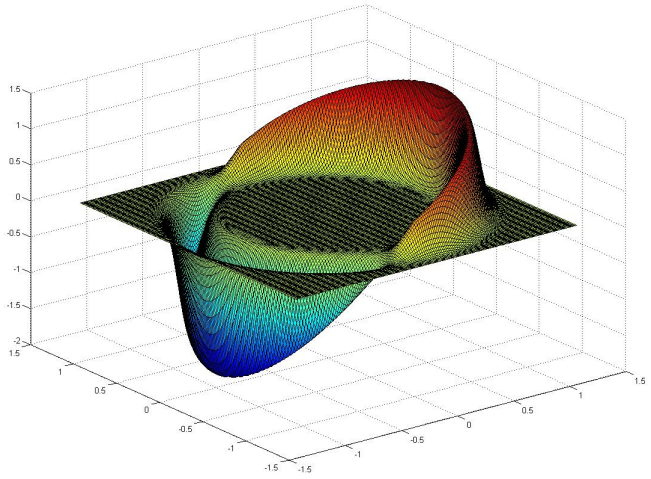

Figure 5: Second eigenfunction, $\Sigma = S^1$, piecewise constant $a(x)$, $\frac{1}{\epsilon} = 200$.

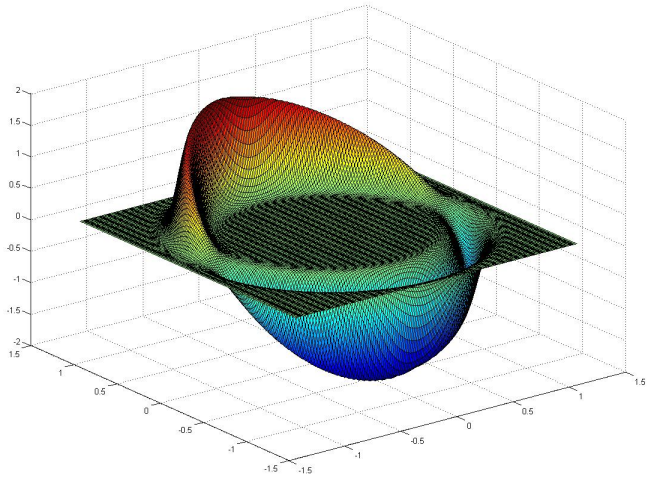

Figure 6: Third eigenfunction, $\Sigma = S^1$, piecewise constant $a(x)$, $\frac{1}{\epsilon} = 200$.

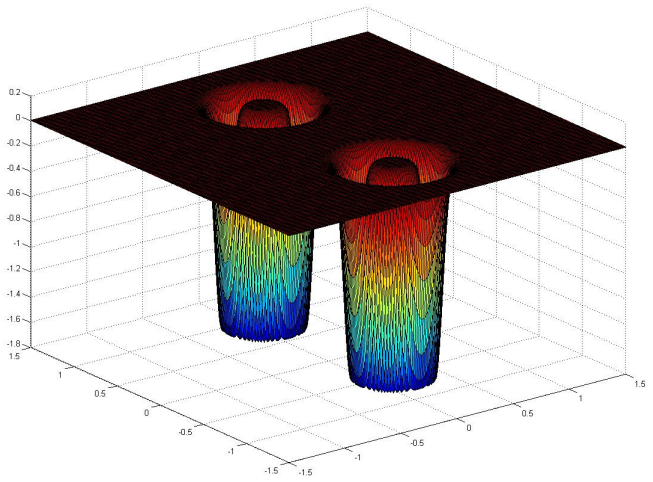

Figure 7: First eigenfunction, $\Sigma =$ union of two circles, $a(x) \equiv 1$, $\frac{1}{\epsilon} = 400$.

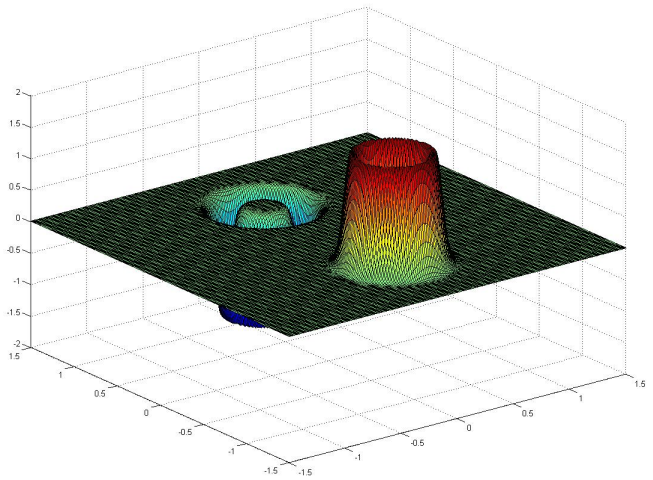

Figure 8: Second eigenfunction,$\Sigma =$ union of two circles, $a(x) \equiv 1$, $\frac{1}{\epsilon} = 400$.

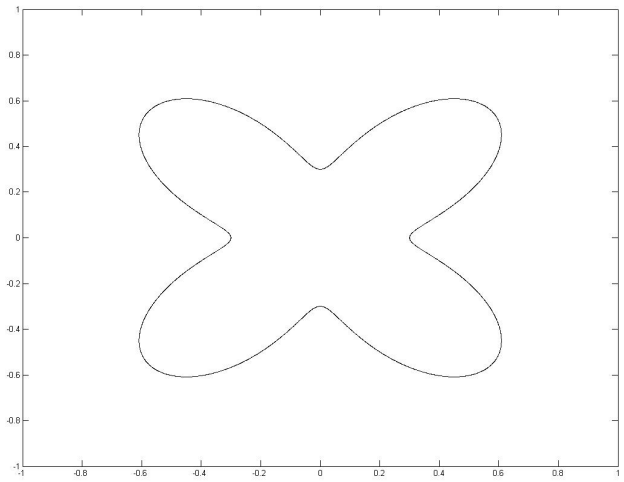

Figure 9: The flower $r(\theta) = 2\cos^2(\theta)\sin^2(\theta) + .3$.

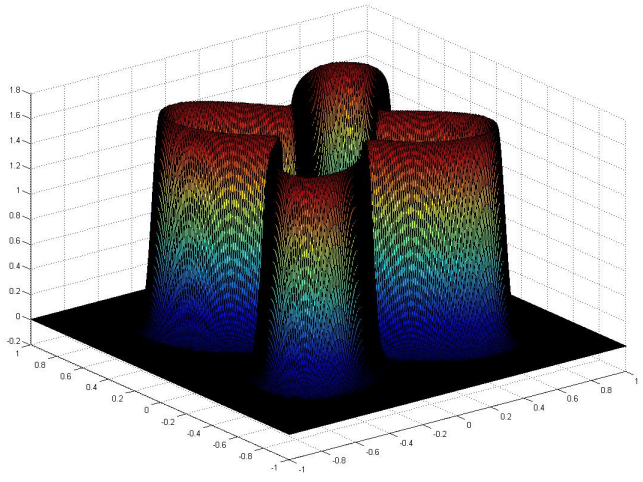

Figure 10: First eigenfunction, $\Sigma =$ flower, $a(x) \equiv 1$, $\frac{1}{\epsilon} = 800$

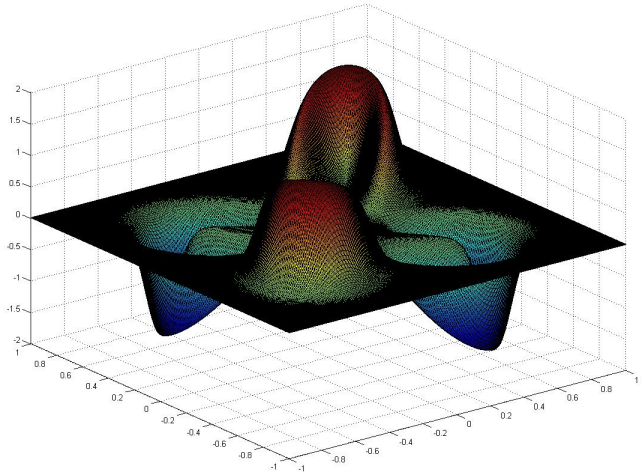

Figure 11: Fifth eigenfunction, $\Sigma =$ flower, $a(x) \equiv 1$, $\frac{1}{\epsilon} = 200$

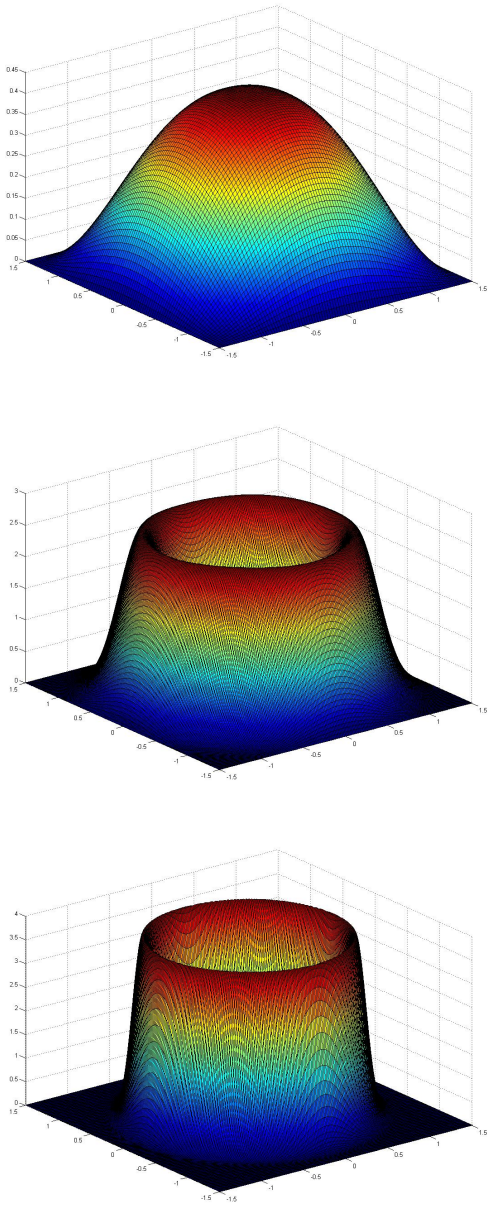

Figure 12: The effect of the parameter ϵ: displayed are the first eigenfunction for $\Sigma = S^1$ and $\frac{1}{\epsilon} = 1, 20, 100$.

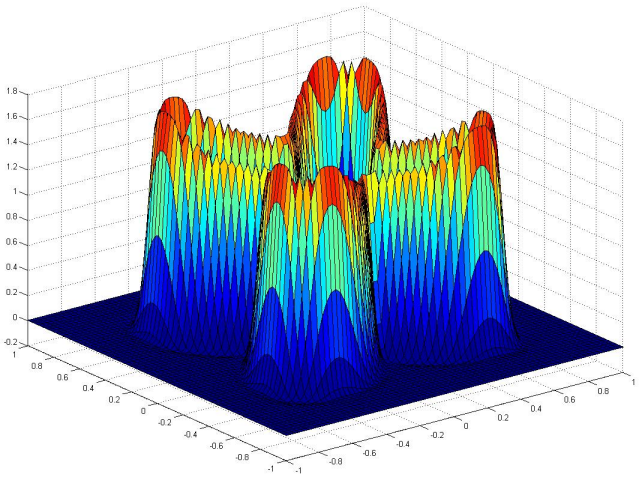

Figure 13: The importance of choosing dx properly. Displayed is the fifth eigenfunction for $\Sigma =$ flower, $\frac{1}{\epsilon} = 200$, dx $= 0.0133$

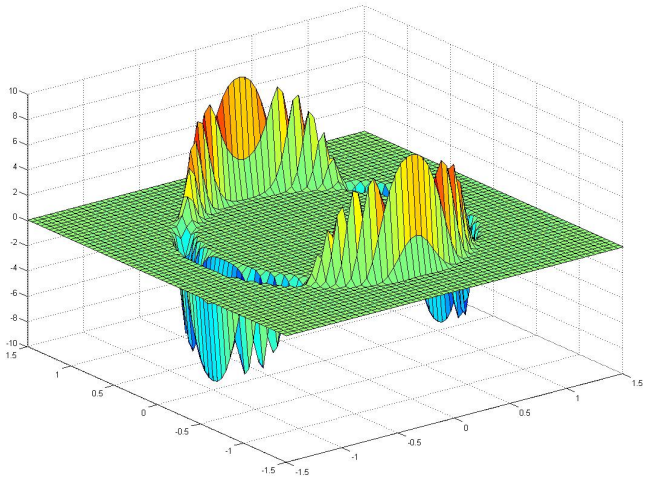

Figure 14: The importance of choosing dx properly. Displayed is the fifth eigenfunction for $\Sigma = S^1$, $\frac{1}{\epsilon} = 800$, dx $= .05$